

Enhancing postmenopausal osteoporosis: a study of KLF2 transcription factor secretion and PI3K-Akt signaling pathway activation by PIK3CA in bone marrow mesenchymal stem cells

Wenjie Ma, Chen Li

Department of Endocrinology, Qilu Hospital (Qingdao), Cheeloo College of Medicine, Shandong University, Qingdao, China

Submitted: 20 June 2023; **Accepted:** 2 September 2023

Online publication: 15 May 2024

Arch Med Sci 2024; 20 (3): 918–937
DOI: <https://doi.org/10.5114/aoms/171785>
Copyright © 2024 Termedia & Banach

Corresponding author:

Chen Li
Department of Endocrinology
Qilu Hospital (Qingdao)
Cheeloo College
of Medicine
Shandong University
Qingdao 266035
China
E-mail: lichenqd0108@126.com

Abstract

Introduction: Mesenchymal stem cells can develop into osteoblasts, making them a promising cell-based osteoporosis treatment. Despite their therapeutic potential, their molecular processes are little known. Bioinformatics and experimental analysis were used to determine the molecular processes of bone marrow mesenchymal stem cell (BMSC) therapy for postmenopausal osteoporosis (PMO).

Material and methods: We used weighted gene co-expression network analysis (WGCNA) to isolate core gene sets from two GEO microarray datasets (GSE7158 and GSE56815). GeneCards found PMO-related genes. GO, KEGG, Lasso regression, and ROC curve analysis refined our candidate genes. Using the GSE105145 dataset, we evaluated KLF2 expression in BMSCs and examined the link between KLF2 and PIK3CA using Pearson correlation analysis. We created a protein-protein interaction network of essential genes involved in osteoblast differentiation and validated the functional roles of KLF2 and PIK3CA in BMSC osteoblast differentiation *in vitro*.

Results: We created 6 co-expression modules from 10 419 differentially expressed genes (DEGs). PIK3CA, the key gene in the PI3K-Akt pathway, was among 197 PMO-associated DEGs. KLF2 also induced PIK3CA transcription in PMO. BMSCs also expressed elevated KLF2. BMSC osteoblast differentiation involved the PI3K-Akt pathway. *In vitro*, KLF2 increased PIK3CA transcription and activated the PI3K-Akt pathway to differentiate BMSCs into osteoblasts.

Conclusions: BMSCs release KLF2, which stimulates the PIK3CA-dependent PI3K-Akt pathway to treat PMO. Our findings illuminates the involvement of KLF2 and the PI3K-Akt pathway in BMSC osteoblast development, which may lead to better PMO treatments.

Key words: postmenopausal osteoporosis, osteoblast differentiation, WGCNA, GEO, Lasso regression analysis, PIK3CA, KLF2, PI3K-Akt pathway.

Introduction

Osteoporosis (OP) is a metabolic bone disease characterized by low bone mass and alterations in bone microstructure, leading to increased bone fragility and a higher risk of fractures [1]. Postmenopausal osteoporosis (PMO) is a prevalent skeletal disorder in postmenopausal women [2, 3]. This systemic disease is featured by the deficiency of bone mass

and elevated bone fracture risk [4]. Ageing, estrogen deficiency, prolonged calcium deficiency, and smoking are strong independent risk factors for PMO [5, 6]. The alleviation of complications associated with PMO is a challenging task to obtain [7, 8]. Of note, the imbalance between the osteogenic and osteoclastic activities is a contributor to osteoporosis [9]. Mesenchymal stem cells (MSCs) are regarded as multipotent cells which can differentiate into osteoblasts, but this compromised ability can cause bone disorders, including osteoporosis [10]. Reduced osteogenesis can be observed in bone marrow mesenchymal stem cells (BMSCs) in patients with osteoporosis [11]. In postmenopausal women, insufficient bone formation by osteoblasts from BMSCs is responsible for osteoporosis [12]. Therefore, it is significant to seek novel targets [13] for regulating osteoblast osteogenesis to treat PMO.

In the present study, weighted gene co-expression network analysis (WGCNA) combined with GEO database-based differential analysis and least absolute shrinkage and selection operator (LASSO) regression analysis identified phosphatidylinositol-4,5-bisphosphate 3-kinase catalytic subunit α (PIK3CA) as the core gene of the PI3K-Akt pathway affecting PMO. PIK3CA can encode the p110 α catalytic subunit of PI3K and assist the PI3K/Akt pathway to regulate important cellular functions [14]. Of note, PIK3CA was identified as a hub protein that might have an impact on the progression of osteoporosis [15]. PIK3CA/Akt/GSK3 β / β -catenin signaling could be activated by icariin, thereby supporting the protection against glucocorticoid-induced osteoporosis [16]. It should be noted that our bioinformatics analysis screened Kruppel-like factor 2 (KLF2) as the potential regulator of PIK3CA. KLF2 is recognized as a zinc finger transcription factor [17]. As previously reported, KLF2 expression could be increased by BMSC-derived extracellular vesicles (EVs) carrying miR-15b, which facilitated osteoblast differentiation [18]. KLF2 downregulation could elevate osteoclast differentiation while suppressing osteoblast differentiation [19]. KLF2 expression could be induced by anti-resorptive bisphosphonates, which are applied for treating osteoporosis [20]. Accumulating evidence has suggested the interaction between KLF2 and the PI3K-Akt pathway [21, 22]. Activation of the PI3K/Akt pathway was suggested to be involved in osteoblast differentiation of MSCs [23]. Strikingly, a previous study revealed that activation of the PI3K-Akt pathway due to miR-483-5p silencing could ameliorate PMO [24].

Given the reports mentioned above, we hypothesized in the present study that the BMSC-secreted transcription factor KLF2 might affect osteoblast differentiation of BMSCs in PMO

by regulating PIK3CA and the PI3K-Akt pathway. This study sheds light on the potential of MSCs in managing PMO through the identification of molecular mechanisms regulating osteoblast differentiation.

Material and methods

GEO microarray data acquisition

Osteoporosis expression profile datasets GSE7158 and GSE56815, and the BMSC-related dataset GSE105145 were obtained through the GEO database. Among them, the GSE7158 dataset included 14 normal control samples and 12 osteoporosis patient samples, the GSE56815 dataset included 20 normal control samples and 20 osteoporosis patient samples, and the GSE105145 dataset included 3 samples of BMSCs and 3 dental pulp MSC samples.

Datasets GSE7158 and GSE56815 were further merged and the ComBat function of the package *sva* was used to correct batch effects. All analyses in this paper were performed under R version 4.2.1.

Differential gene expression analysis

Differential analysis was performed through the “limma” package of R language, selecting the differentially expressed genes (DEGs) in each dataset with $|\log_{2}FC| > 1$ and $p < 0.05$ as the screening condition. Volcano maps were drawn using the “ggplot2” package of R language and differential gene expression heat maps were drawn using the “heatmap” package.

WGCNA

To further understand the interrelationship between the merged genes from the GSE7158 and GSE56815 datasets, and to identify the central genes of the gene modules, the co-expression network of osteoporosis samples was constructed with the WGCNA algorithm. The sample cluster analysis was performed using the R language “hclust” package. Gene co-expression networks were constructed using the R language “WGCNA” package. First, the expression of individual genes was transformed into a similarity matrix based on the Pearson correlation coefficient between pairs of genes. A hierarchical clustering dendrogram was constructed using an expression matrix to detect outliers. Then, the scale-free topological fitting exponent was calculated as a function of soft threshold power based on the network topological analysis function. The topological overlap matrix-based dissimilarity measure was then used to calculate the connectivity between genes in the module with similar expression profiles, and hierarchical clustering was utilized to produce a hier-

archical clustering dendrogram of genes. Finally, a dynamic mixed cutting method was used to divide these genes into different modules.

Gene selection by GeneCards analysis

Genes associated with “PMO” and “osteoblast differentiation” were searched by the GeneCards database and ranked by the Relevance score from high to low. The selected genes were imported into the STRING database for protein-protein interaction (PPI) analysis, where the “species” was limited to “human”. The PPI network of regulatory relationship was drawn through the Cytoscape software (v3.6.0).

Gene functional enrichment analysis

The analysis results were intersected using the R language “VennDiagram” package, and a Venn diagram of the intersected DEGs was obtained. GO (biological processes, cellular components, and molecular functions) and KEGG enrichment analyses were performed using the R language “ClusterProfiler” package. The cellular functions and pathways mainly affected by potential targets and key targets were analyzed. $p < 0.05$ was considered statistically significant.

Lasso regression analysis

Regression analysis is a mathematical model that constructs quantitative relationships between variables based on determining the dependent and independent variables. The “glmnet ()” function package in R Studio software was called to load the candidate gene matrix. When $\alpha = 1$, the appropriate λ value was selected, and the internal validation was implemented by the ten-fold cross-validation method to determine the best model.

$$\frac{1}{2m} \left[\sum_{i=1}^m (h_0(x^{(i)}) - y^{(i)})^2 + \lambda \sum_{j=1}^k |w_j| \right]$$

M – number of samples, k – number of parameters, λ – regularization parameters.

Receiver operating characteristic (ROC) analysis

The “pROC ()” function in the R Studio software was used to draw the ROC curve for the model. The overall survival (OS) included in the data was selected as the dependent variable. With the specificity as the horizontal axis and the sensitivity as the vertical axis, the ability of the AUC evaluation model to distinguish the risk of PMO prognosis was calculated. In the case of $AUC > 0.5$, the closer the AUC was to 1, the better the model could predict the PMO prognosis.

Cell culture and treatment

Human bone marrow mesenchymal stem cell line UE7T-13 (Biobw, Beijing, China) was cultured in RPMI-1640 medium (11875093, Gibco) containing 10% fetal bovine serum (FBS; 10099141, Gibco), and 1% penicillin/streptomycin (SV30010, Gibco) at 37°C under 5% CO₂. Then cells were transfected with siRNA plasmids (HanBio, Shanghai, China) targeting PIK3CA (PIK3CA-si) and KLF2 (KLF2-si) as well their corresponding NC (PIK3CA-si-NC and KLF2-si-NC) using Lipofectamine 3000 reagents (L3000015, Invitrogen). The normal cells were cultured with normal culture medium while the remaining cells were cultured with the osteogenic induction medium (#HUXMX-90021, Cyagen Bioscience Inc., Suzhou, Jiangsu, China). siRNA sequences are shown in Supplementary Table SI.

Cell differentiation determination

To induce osteoblast differentiation, BMSCs (1×10^5) were cultured in a endothelial cells (ECs) were cultured on 0.1% gelatin-coated coverslips in 24-well culture plates and osteogenic induction medium (HUXMX-90021, Cyagen) for 1 week. Alkaline phosphatase (ALP) staining and alizarin red-S (ARS) staining were carried out using an Alkaline Phosphatase Assay Kit (P0321S, Beyotime, Shanghai, China) and alizarin red-S solution (C0148S, Beyotime), respectively.

RT-qPCR

Total RNA was extracted from cells and tissues via homogenization in TRIzol reagent (10296010, Thermo Fisher Scientific Inc., Waltham, MA; 1 ml per 100 mg tissues), addition of chloroform (200 ml), and centrifugation at 12000 g and 4°C for 10 min. The upper aqueous phase was collected and mixed with 500 ml of isopropanol to precipitate the RNA. RNA was dissolved in RNase-free water (10–30 ml) and quantified on a NanoDrop ND-3300 Spectrophotometer (Thermo Fisher Scientific Inc.). The RNA (1 mg) was reverse transcribed using TaqMan Reverse Transcription Kit (N8080234, Thermo Fisher Scientific Inc.), and qPCR was performed using PowerUp SYBR Green Master Mix (Thermo Fisher Scientific Inc., A25741). GAPDH and U6 were regarded as internal references and the fold changes were calculated by relative quantification ($2^{-\Delta\Delta Ct}$ method). The primer sequences are shown in Supplementary Table SII.

Western blot

Total protein was extracted, separated and transferred onto membranes. The membrane was blocked using TBST (5 ml) with 5% skimmed milk powder (P0216-300 g, Beyotime) and underwent

overnight incubation at 4°C with primary antibodies to PIK3CA (p110 & p85) (51 kDa, #ab40776, Abcam, Cambridge, UK), KLF2 (139 kDa, #ab236507, Abcam), Akt1 (56 kDa, #ab238477, Abcam), p-Akt1 (56 kDa, #ab81283, Abcam), collagen I (139 kDa, #ab138492, Abcam), ALP (39 kDa, #ab307726, Sigma), RUNX2 (57 kDa, #ab236639, Abcam), OCN (11 kDa, #ab133612, Abcam), and GAPDH (36 kDa, #PA1-987, Thermo Fisher Scientific Inc.). The next day, the membrane was incubated with HRP-labeled secondary antibody goat anti-rabbit (A0208, Beyotime). ECL (P0018FS, Beyotime) was used for chemiluminescence detection and membranes were photographed by the ChemiDoc XRS+ system (Bio-Rad). The band intensity was quantified using Image J analysis software, normalized to GAPDH [25].

ChIP assay

BMSCs cultured in the osteogenic induction medium for 1 week were collected and probed with antibodies to KLF2 (139 kDa, #ab236507, Abcam) and IgG (52 kDa, #ab109489, Abcam, serving as a NC). The primers used for this assay are shown in Supplementary Table SIII [26].

Statistical analysis

The Wilcoxon test was used to compare differences between the two sets of non-normally distributed data. The unpaired *t*-test was used to compare differences between two sets of normally distributed data. The Pearson correlation analysis was performed to compare the correlation between the two data groups and to calculate the correlation coefficients. The R software (4.2.1), SPSS (22.0), and Prism were used for statistical analysis and mapping. $p < 0.05$ demonstrated that the difference was statistically significant.

Results

GEO-based differential analysis for screening DEGs in PMO

In order to find the molecular mechanisms to alleviate PMO, differential analysis and WGCNA through GSE7158 and GSE56815 datasets were performed. In combination with the GeneCards website, Lasso regression analysis and ROC curve analysis were carried out, and the biological function of core genes was analyzed by functional enrichment. The BMSC-related dataset GSE105145 was used to screen the transcription factors involved in the regulation, and a PPI regulatory network was constructed to provide a theoretical basis for further understanding the mechanism of PMO and finding potential diagnosis and treatment targets. The bioinformatics analysis process is shown in Supplementary Figure S1.

To screen DEGs in PMO, differential analysis was performed using the combined dataset of GSE7158 and GSE56815. A total of 10419 DEGs were selected, where 8308 DEGs were downregulated, and 2112 DEGs were upregulated (Figures 1 A, B).

WGCNA-based screening for the green core module

First, 12530 genes in the expression profiles of the combined dataset of GSE7158 and GSE56815 were selected for cluster evaluation, and a total of 66 samples were used for subsequent WGCNA (Figure 2 A). The best value of the soft threshold (power) was set to 14 to build a gene expression network (Figure 2 B).

Modules with high similarity of module eigengenes were merged by dynamic mixed clipping method, where the minModules size was set to 30, deepSplit to the default value of 2, and cut height to 0.25. Each module was shown in a different color (Figure 3 A). Pearson correlation analysis was performed between each module eigengene and different groups (Figure 3 B). The six co-expression modules with the top absolute value of the correlation coefficient and *p* value were selected for subsequent analysis, including the green module (2647 genes), the black module (4413 genes), the purple module (99 genes), the magenta module (241 genes), the pink module (824 genes) and the grey module (4281 genes). Among them, the green module showed the most significant correlation ($cor = 0.76$, $p < 1e-200$) (Figure 3 C).

Identification of 197 core DEGs related to PMO

GEO-based differential analysis was performed to screen PMO-related DEGs. The WGCNA screened core green module-related DEGs for Venn analysis, and 2189 common DEGs (Figure 4 A) were obtained. Through the GeneCards website, 1188 PMO-related genes were further screened to intersect with 2189 DEGs, and 197 candidate DEGs related to PMO progression were obtained (Figure 4 B).

The candidate DEGs were subjected to KEGG and GO functional enrichment analyses. The results of the KEGG pathway analysis showed that the candidate DEGs were mainly enriched in the PI3K-Akt pathway, cytokine-cytokine receptor interaction, Jak-STAT pathway, and Th17 cell differentiation pathway (Figure 4 C). The results of GO functional analysis revealed that the candidate DEGs were mainly enriched in ossification, response to peptide, organic hydroxy compound metabolic process and multicellular organismal homeostasis in biological processes. The candidate DEGs were mainly enriched in the collagen-containing extracellular matrix, extracellular

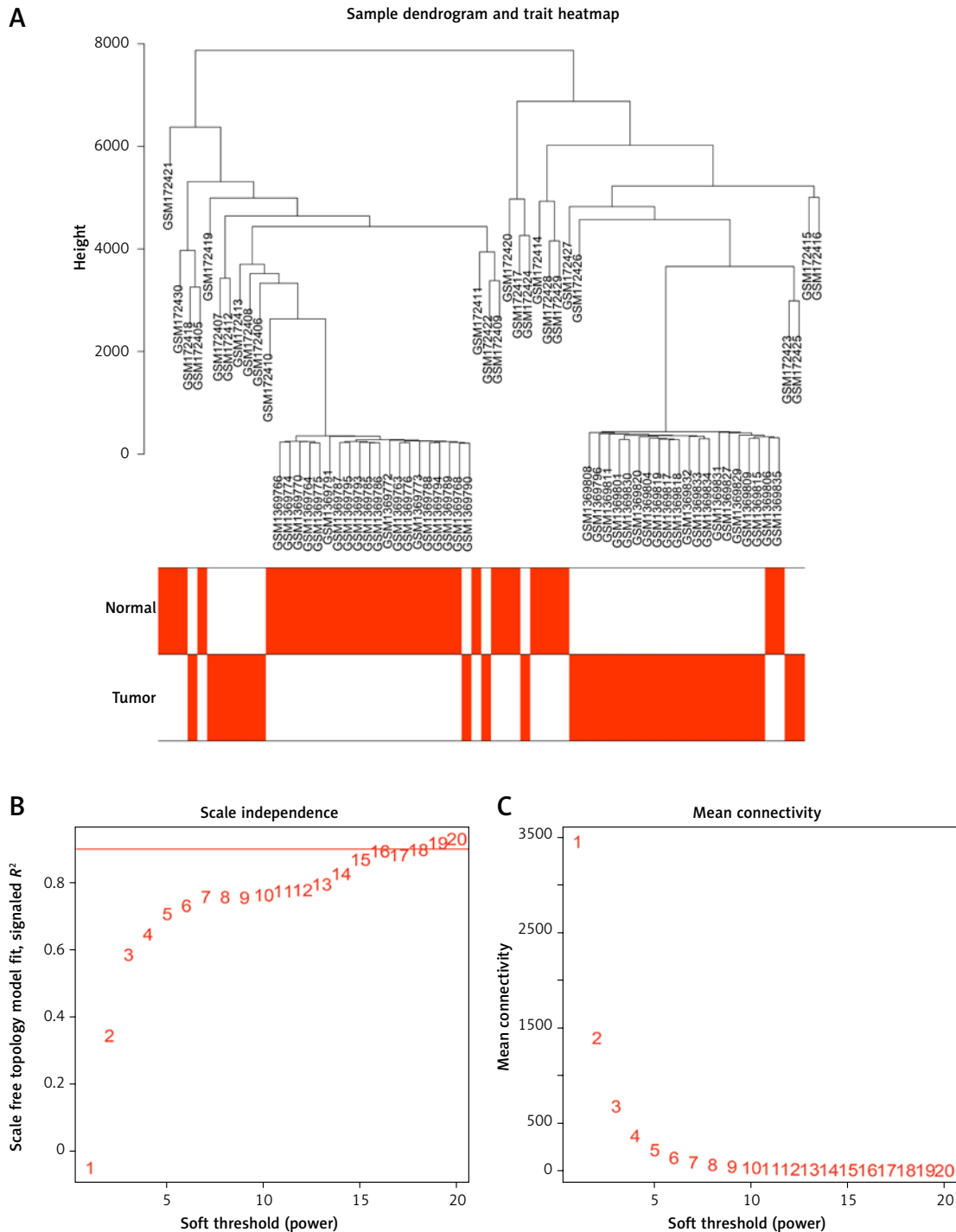


Figure 2. Data validation and screening for optimal soft thresholds. **A** – Heterogeneity viewed by sample clustering. **B** – Non-scale fitting index analysis of soft threshold. **C** – Analysis of soft threshold average connectivity

matrix, blood microparticle, and secretory granule lumen in cellular components. The candidate DEGs were mainly enriched in receptor regulator activity, receptor ligand activity, growth factor activity, and cytokine receptor binding in molecular function (Figures 4 D–F).

The above results suggested that the candidate DEGs mainly played roles in ossification and cytokine regulation, and were enriched in extracel-

lular matrix and vesicles. The molecular functions of candidate DEGs were mainly related to cytokine-related enzyme activity and receptor activity. According to the results of the KEGG analysis, the candidate DEGs were involved in the regulation of the PI3K-Akt pathway. It has been found that the activation of the PI3K-Akt pathway could regulate the bone balance of PMO, inhibit osteoblast apoptosis and promote cell proliferation [27]. There-

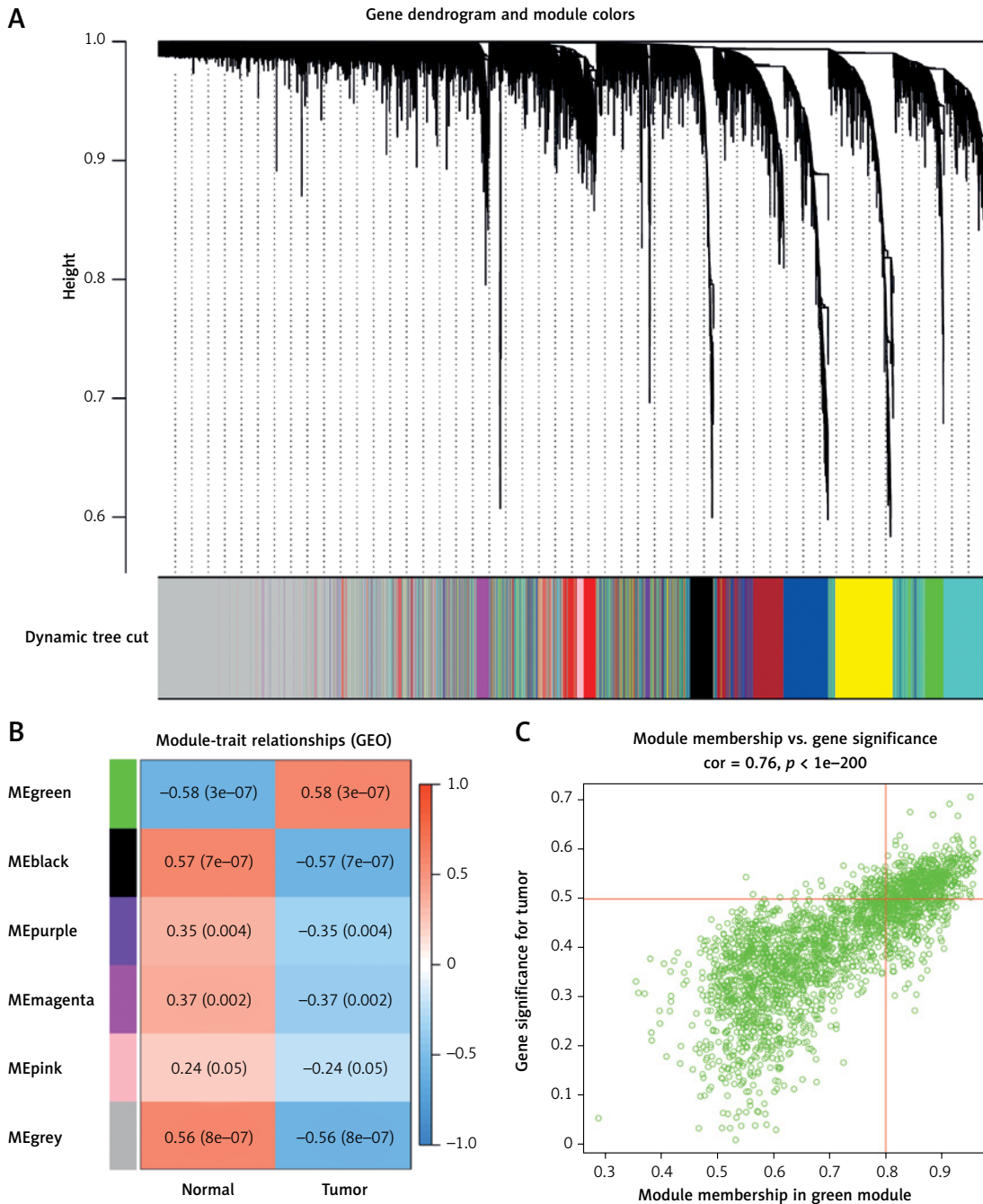


Figure 3. Co-expression network constructed based on the combined dataset of GSE7158 and GSE56815. **A** – Gene dendrogram. **B** – Pearson correlation analysis between each module eigengene and different groups. **C** – Correlation coefficient of the green module

fore, we further investigated the molecular regulatory mechanism of the PI3K-Akt pathway in PMO.

PIK3CA as the core gene of the PI3K-Akt pathway affecting PMO

To further investigate the core regulatory genes in candidate DEGs, we performed Lasso regression analysis of the 14 related genes involved in the PI3K-Akt pathway (GHR, ATF2, IL4R, COL2A1, IRS1, FGF18, JAK2, CSF1, HSP90AA1, FLT3, MAPK3,

PIK3CA, CCND1, and MTOR) in the candidate DEGs. The Lasso algorithm used the L1 criterion for model construction, and the change of the regression coefficient under the L1 criterion is shown in Figure 5 A. With a parameter $\alpha = 1$, ten-fold cross-validation was used for model internal validation. The selection process diagram of the cross-validation parameter λ was drawn, where the $\log(\lambda)$ was indicated on the horizontal axis and the root mean square error value (RMSE) on the vertical axis (Figure 5 B). When the model

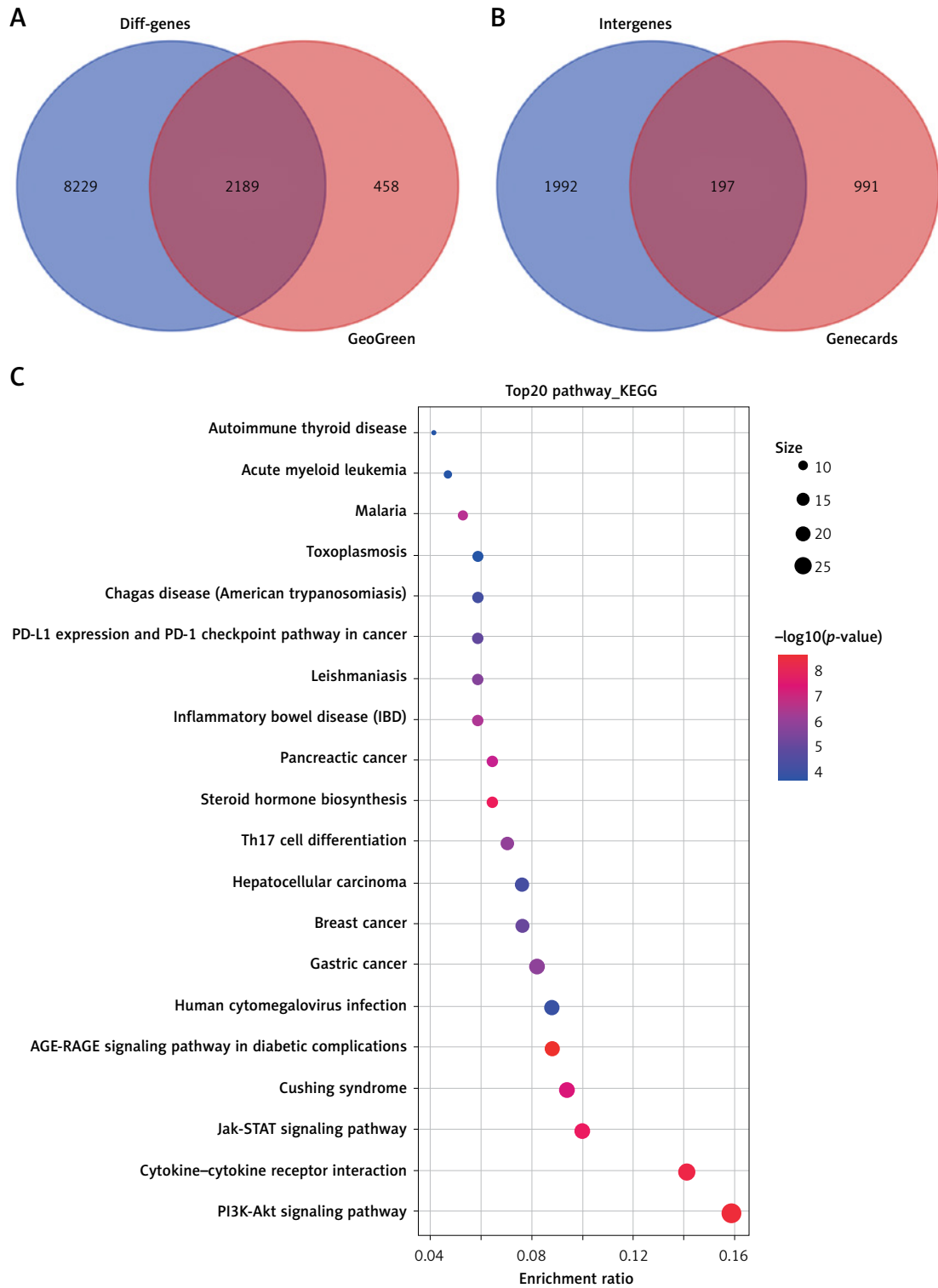


Figure 4. Screening for core DEGs and regulatory function analysis. **A** – Venn diagram of the green module-related DEGs and DEGs in GEO database. **B** – Venn diagram of PMO-related genes and 2189 DEGs. **C** – KEGG pathway enrichment analysis of candidate DEGs

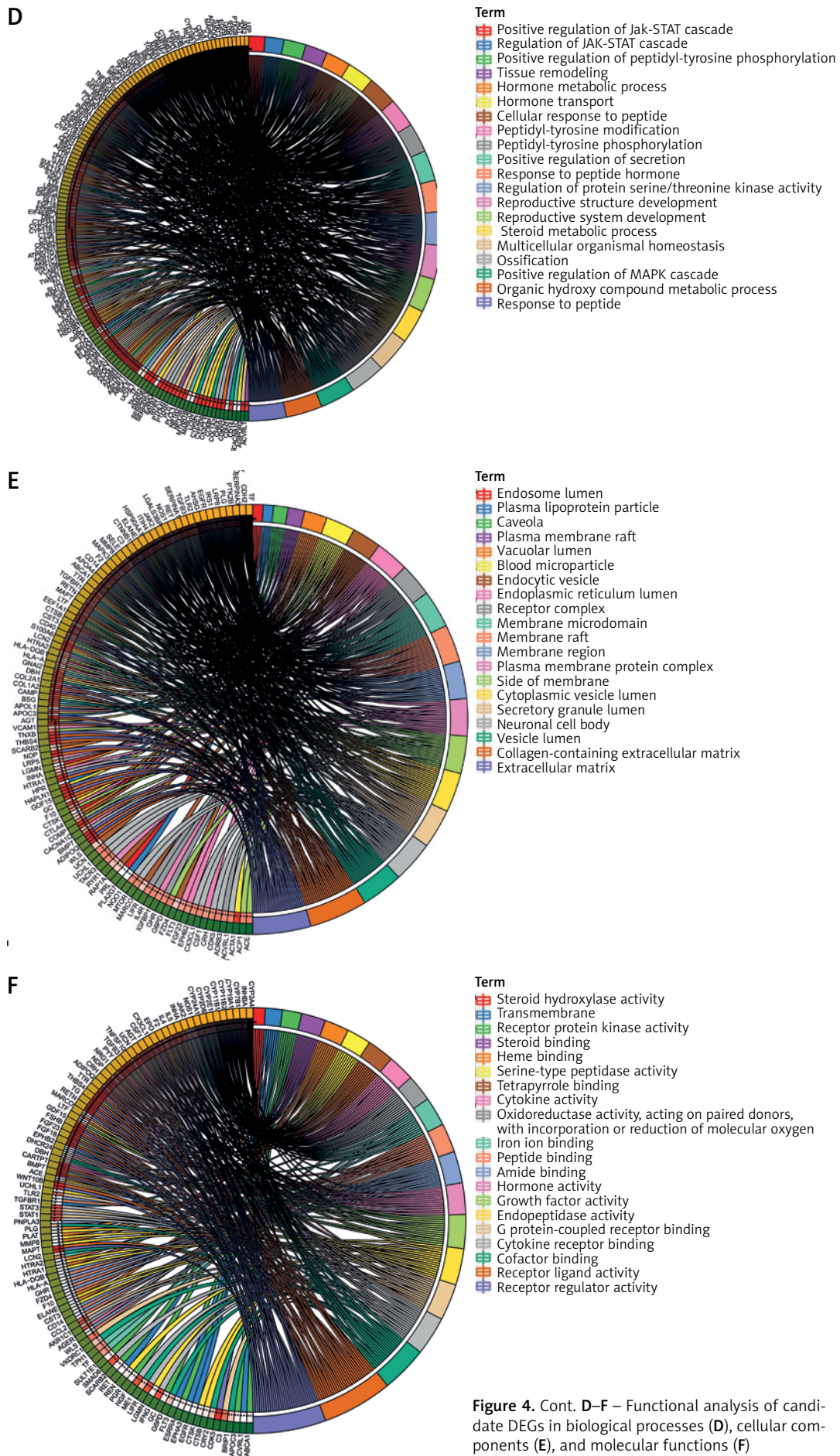


Figure 4. Cont. **D–F** – Functional analysis of candidate DEGs in biological processes (**D**), cellular components (**E**), and molecular functions (**F**)

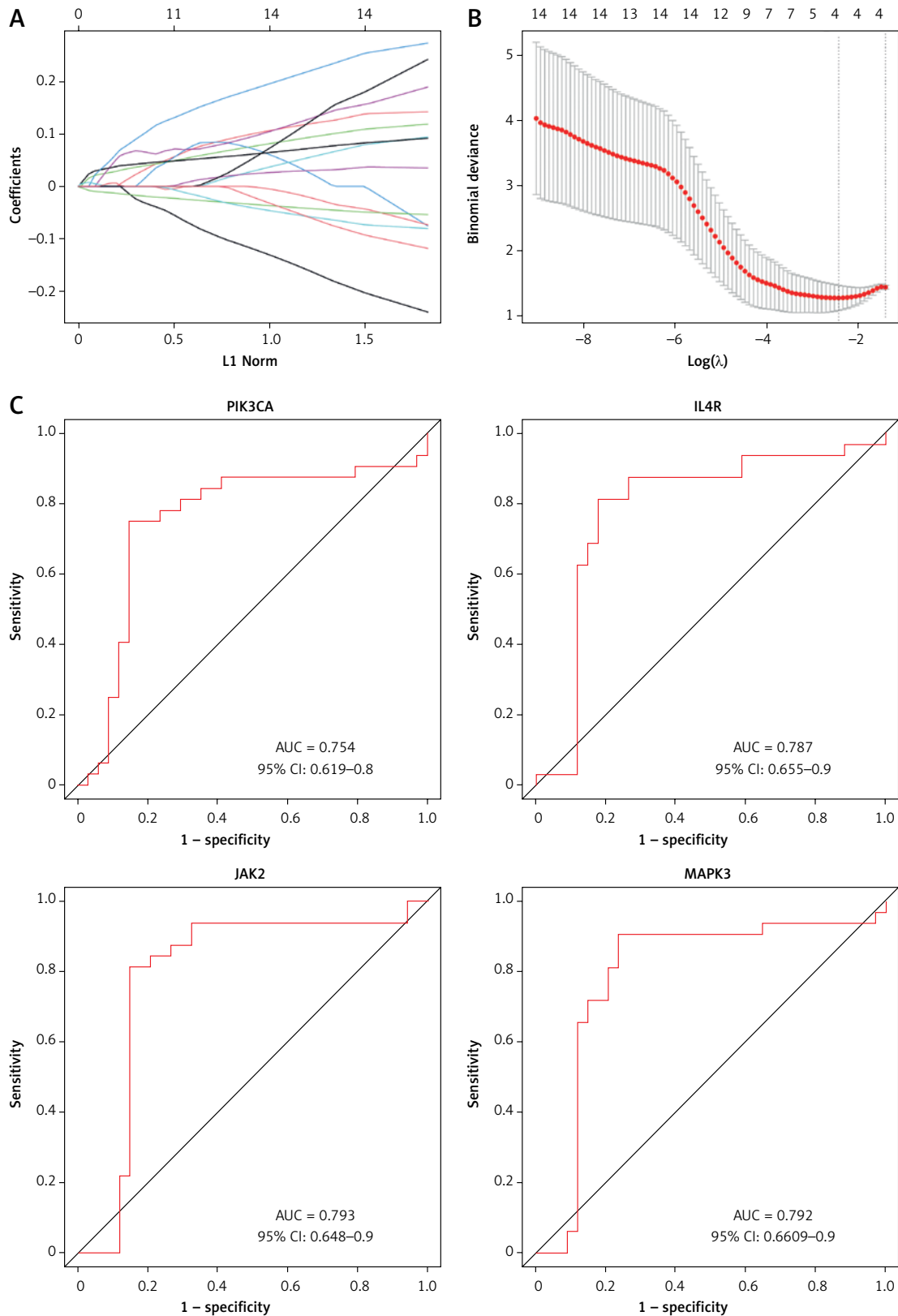


Figure 5. Screening for the core genes of the PI3K-Akt pathway affecting PMO. **A** – Lasso regression analysis of candidate DEGs and regression coefficient variation diagram under L1 criterion. **B** – Selection process diagram of cross-validation parameter λ . **C** – ROC curve diagram of 4 candidate DEGs

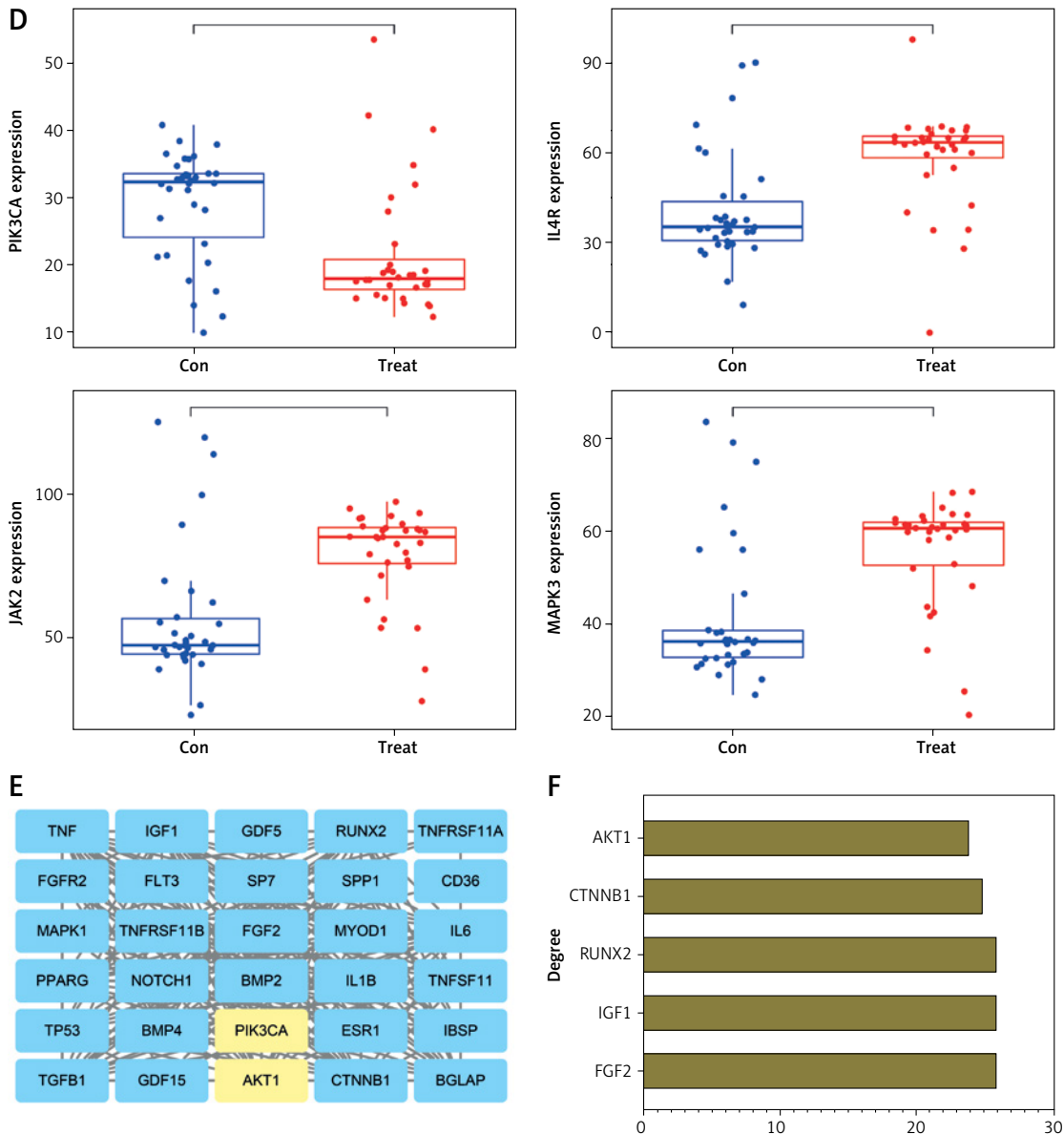


Figure 5. Cont. **D** – Boxplot of the expression of 4 candidate DEGs in the combined dataset of GSE7158 and GSE56815. **E** – Construction of a PPI network of the top 30 genes related to osteoblast differentiation retrieved from the GeneCards website and core genes of the PI3K-Akt pathway. **F** – Calculation of the degree value of genes in the PPI network

variable value was 4, the RMSE value was minimal; therefore, the corresponding candidate DEGs (PIK3CA, IL4R, JAK2, and MAPK3) were selected for subsequent analysis.

The ROC curves of the four DEGs were drawn, and AUC values were calculated (Figure 5 C). The results showed that the AUC values of PIK3CA, IL4R, JAK2, and MAPK3 were 0.754, 0.787, 0.793, and 0.792, respectively, all of which met $AUC > 0.75$, suggesting that the model had a good discriminatory ability to predict PMO prognosis. Further calculation of PIK3CA, IL4R, JAK2, and MAPK3 expression in PMO showed that PIK3CA was significantly less expressed in the disease group than in the control group. In contrast, the other three

genes showed the opposite trend (Figure 5 D). Therefore, we selected PIK3CA as the core gene to explore the regulatory mechanism of the PI3K-Akt pathway in PMO.

Previous literature has shown that promoting osteoblast differentiation of BMSCs can effectively alleviate PMO [28]. In order to further explore the mechanism, we screened for genes related to osteoblast differentiation through the GeneCards website, and selected the top 30 genes and core genes of the PI3K-Akt pathway to construct a PPI network (Figure 5 E). From the network, we observed that Akt1 and PIK3CA, the core genes of the PI3K-Akt pathway, were closely related to osteoblast differentiation. Further calculation of the

Degree value, which is the most direct measure to characterize node centrality in a network analysis, identified Akt1 to be one of the core genes in the PPI network (Figure 5 F). The above results indicate that the PI3K-Akt pathway can participate in the osteoblast differentiation of BMSCs.

PIK3CA promoted osteoblast differentiation of BMSCs

Having identified PIK3CA as the core gene of the PI3K-Akt pathway affecting PMO, we continued to verify the effect of PIK3CA on the osteoblast differentiation of BMSCs. The mRNA and protein expression of PIK3CA was found to be increased in the BMSCs cultured with osteogenic induction medium versus normal BMSCs (Figures 6 A, B), implying that PIK3CA may facilitate osteoblast differentiation of BMSCs. Subsequently, we designed two siRNA sequences targeting PIK3CA and transfected them into BMSCs. The PIK3CA-si2 sequence showed superior silencing efficiency and was used for subsequent experiments (Figures 6 C, D).

As shown in Figure 6 E, a reduction was noted in the osteoblast differentiation of BMSCs transfected with PIK3CA-si. In addition, the expression of osteoblast differentiation-related proteins collagen I, ALP, RUNX2 and OCN was decreased in BMSCs transfected with PIK3CA-si (Figure 6 F). Meanwhile, silencing of PIK3CA inhibited the phosphorylation level of Akt1 (Figure 6 G). Altogether, these results demonstrate that PIK3CA may be a key gene to facilitate osteoblast differentiation of BMSCs.

The transcription factor KLF2 promoted PIK3CA transcription

The transcription factor is a key molecule of gene expression regulation. To explore whether there was a molecular mechanism of the transcription factor to regulate PIK3CA expression in PMO, 1369 human transcription factors were downloaded through the *humantfs* website to intersect with the top 100 DEGs in PMO, and only the transcription factor KLF2 was obtained (Figure 7 A). Pearson correlation analysis results showed that in the combined dataset of GSE7158 and GSE56815, transcription factor KLF2 was positively correlated with PIK3CA expression (Figure 7 B). Using the JASPAR website, the binding site of the transcription factor KLF2 (Figure 7 C) and that between KLF2 and the PIK3CA promoter region (Supplementary Table SIV) were analyzed.

BMSCs can self-renew and multi-differentiate, and they are indispensable components in osteoblast differentiation and skeletal remodeling in PMO. The process is controlled by a multistep mo-

lecular pathway, and regulated by different transcription factors and signaling proteins. To explore the expression of the transcription factor KLF2 in BMSCs, we performed a differential analysis of the BMSC-related dataset GSE105145 and selected 4510 DEGs, including 2369 upregulated genes and 2141 downregulated genes (Figures 7 D, E). We found that the transcription factor KLF2 was significantly highly expressed in the BMSC samples, compared to that in the control samples (Figure 7 F). It has been well documented that KLF2 promoted the stemness maintenance and self-renewal of BMSCs [29]. Therefore, we could draw the preliminary conclusion that BMSCs might participate in the transcription and development of PMO by regulating PIK3CA transcription through secretion of the transcription factor KLF2.

KLF2 was involved in the osteoblast differentiation of BMSCs by regulating the PI3K-Akt pathway

To verify whether the transcription of PIK3CA is regulated by KLF2, we first detected the expression of KLF2 in BMSCs cultured with osteogenic induction medium by RT-qPCR and Western blot. The results showed an increase of the mRNA and protein expression of PIK3CA in the BMSCs cultured with osteogenic induction medium versus normal BMSCs (Figures 8 A, B). Then, we designed two siRNA sequences targeting KLF2 and transfected them into BMSCs. RT-qPCR and Western blot identified their silencing efficiency, with the KLF2-si1 sequence showing higher silencing efficiency, and it was used for subsequent experiments (Figures 8 C, D).

In the absence of KLF2, osteoblast differentiation of BMSCs (Figure 8 E) was weakened in addition to decreased expression of osteoblast differentiation-related proteins collagen I, ALP, RUNX2 and OCN (Figure 8 F). Meanwhile, silencing of KLF2 inhibited the phosphorylation level of Akt1 (Figure 8 G). Further, ChIP results demonstrated that KLF2 could bind to the promoter region of PIK3CA (Figure 8 H), indicating that the transcription of PIK3CA is regulated by KLF2. Overall, KLF2 can regulate the PI3K-Akt signaling pathway through PIK3CA, thereby promoting the osteoblast differentiation of BMSCs.

Discussion

Postmenopausal-triggered bone loss is mainly attributed to declined core transcription factors of BMSCs [30]. The therapeutic strategy by enhancing osteoblast differentiation is considered as a promising direction for osteoporosis treatment. Herein, we illustrated the mechanistic basis for the anti-osteoporotic effect of BMSCs using bio-

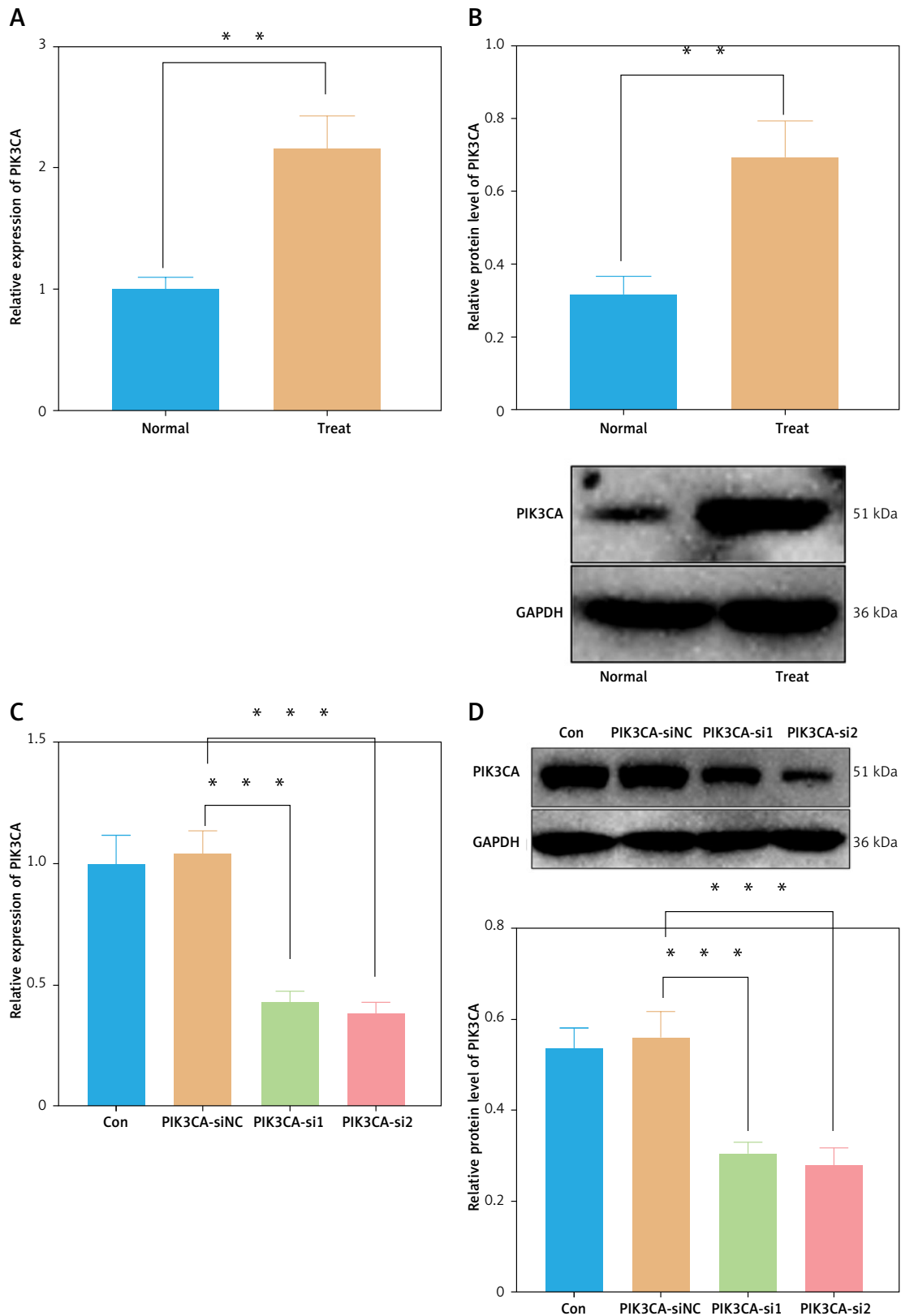


Figure 6. PIK3CA facilitates osteoblast differentiation of BMSCs. **A** – mRNA expression of PIK3CA in the BMSCs cultured with normal medium and osteogenic induction medium detected by RT-qPCR. **B** – Western blot of PIK3CA protein in the BMSCs cultured with normal medium and osteogenic induction medium. **C** – Silencing efficiency of PIK3CA-si in the BMSCs detected by RT-qPCR. **D** – Silencing efficiency of PIK3CA-si in the BMSCs detected by Western blot.

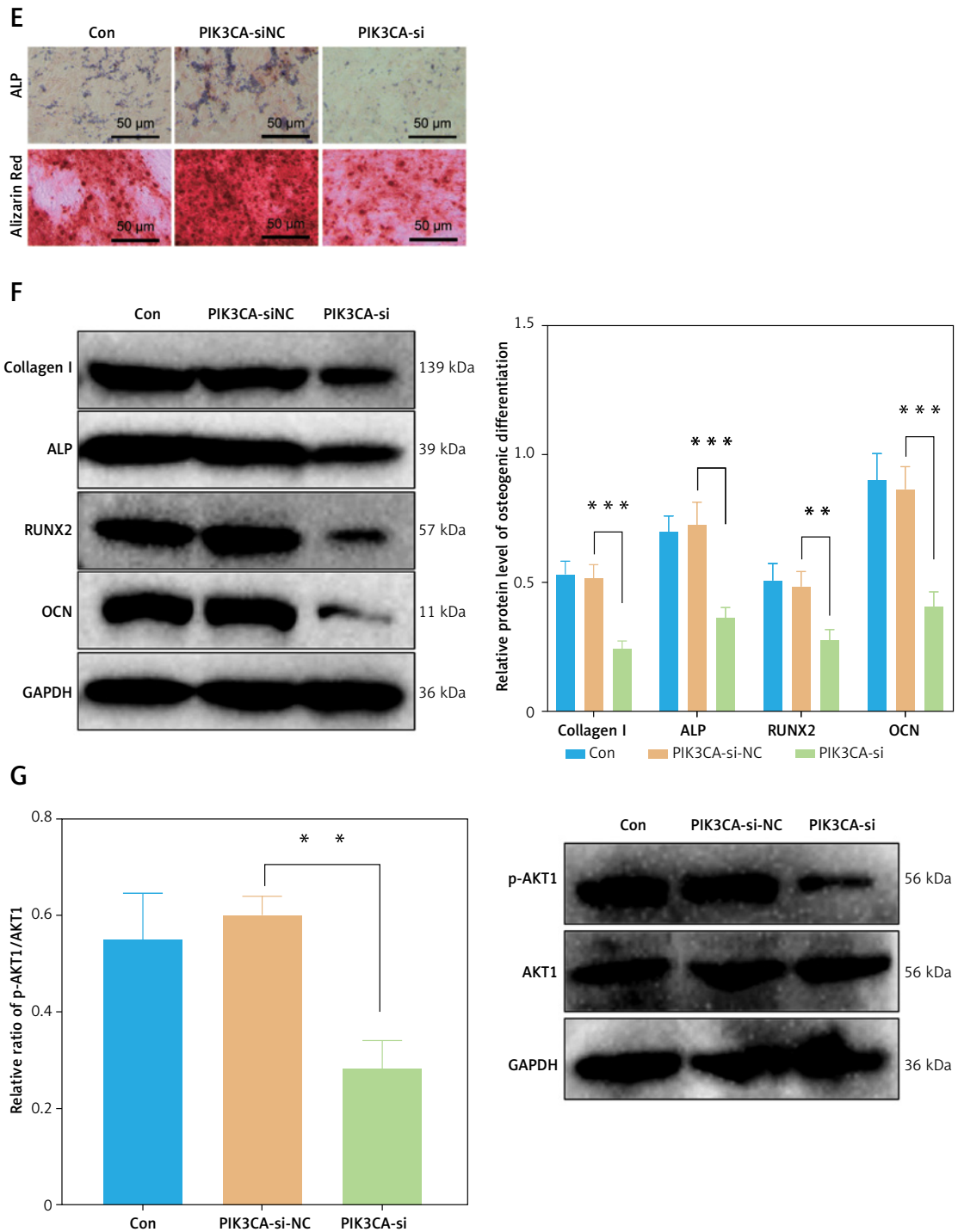


Figure 6. Cont. **E** – Osteoblast differentiation of BMSCs transfected with PIK3CA-si detected by ALP staining and ARS staining. **F** – Western blot of osteoblast differentiation-related proteins collagen I, ALP, RUNX2 and OCN was decreased in BMSCs transfected with PIK3CA-si. **G** – Phosphorylation level of Akt1 in BMSCs transfected with PIK3CA-si detected by Western blot. * $p < 0.05$, ** $p < 0.01$

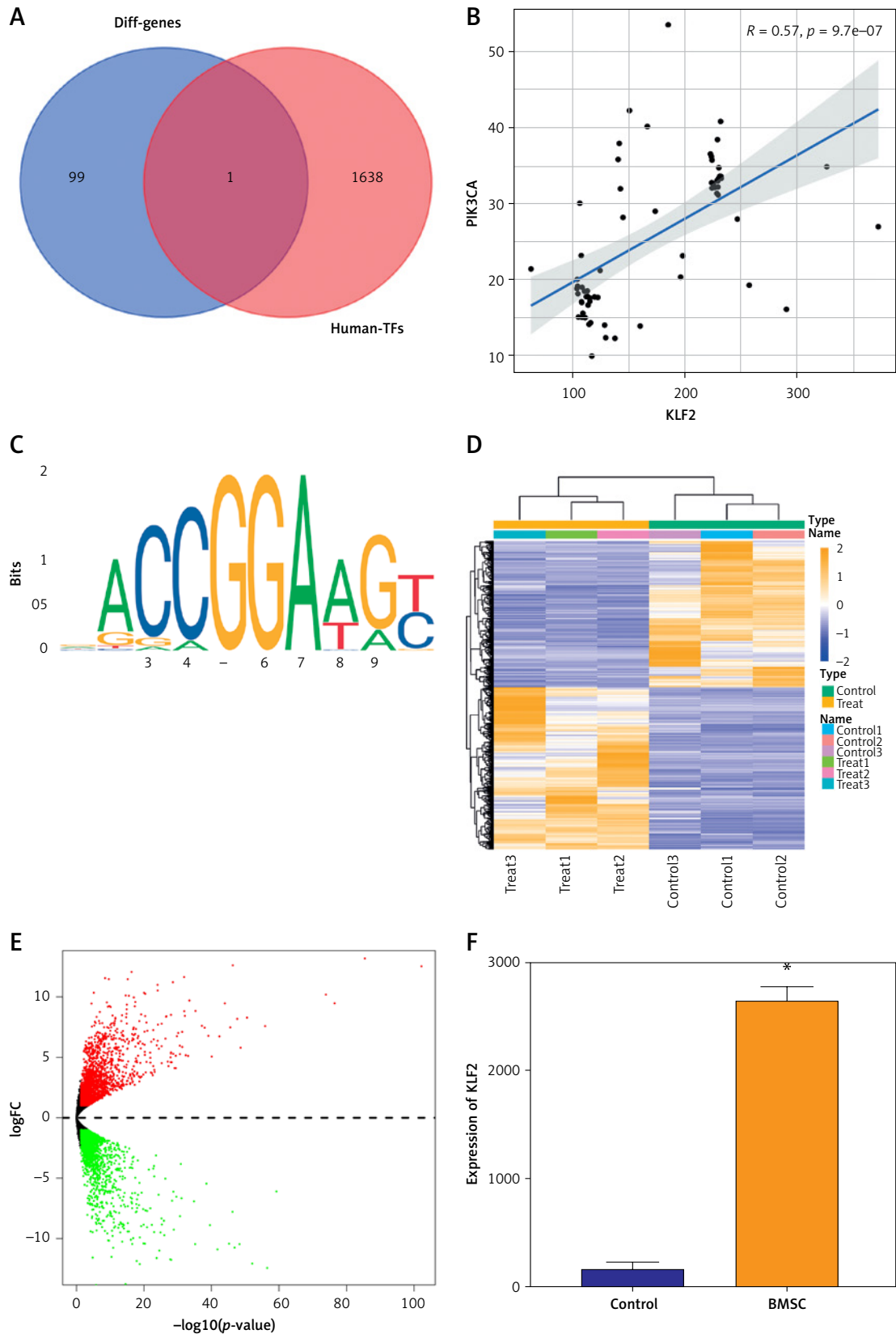


Figure 7. Screening for transcription factors regulating PIK3CA expression. **A** – Venn diagram of DEGs in PMO and human transcription factors. **B** – Pearson correlation analysis of transcription factor KLF2 and PIK3CA. **C** – JASPAR website was used to predict the binding site of transcription factor KLF2. **D** – Heat map of DEGs in the BMSC-related GSE105145 dataset. **E** – Volcano map of DEGs in the BMSC-related GSE105145 dataset. **F** – Expression of transcription factor KLF2 in GSE105145. * $p < 0.05$ vs. the control group

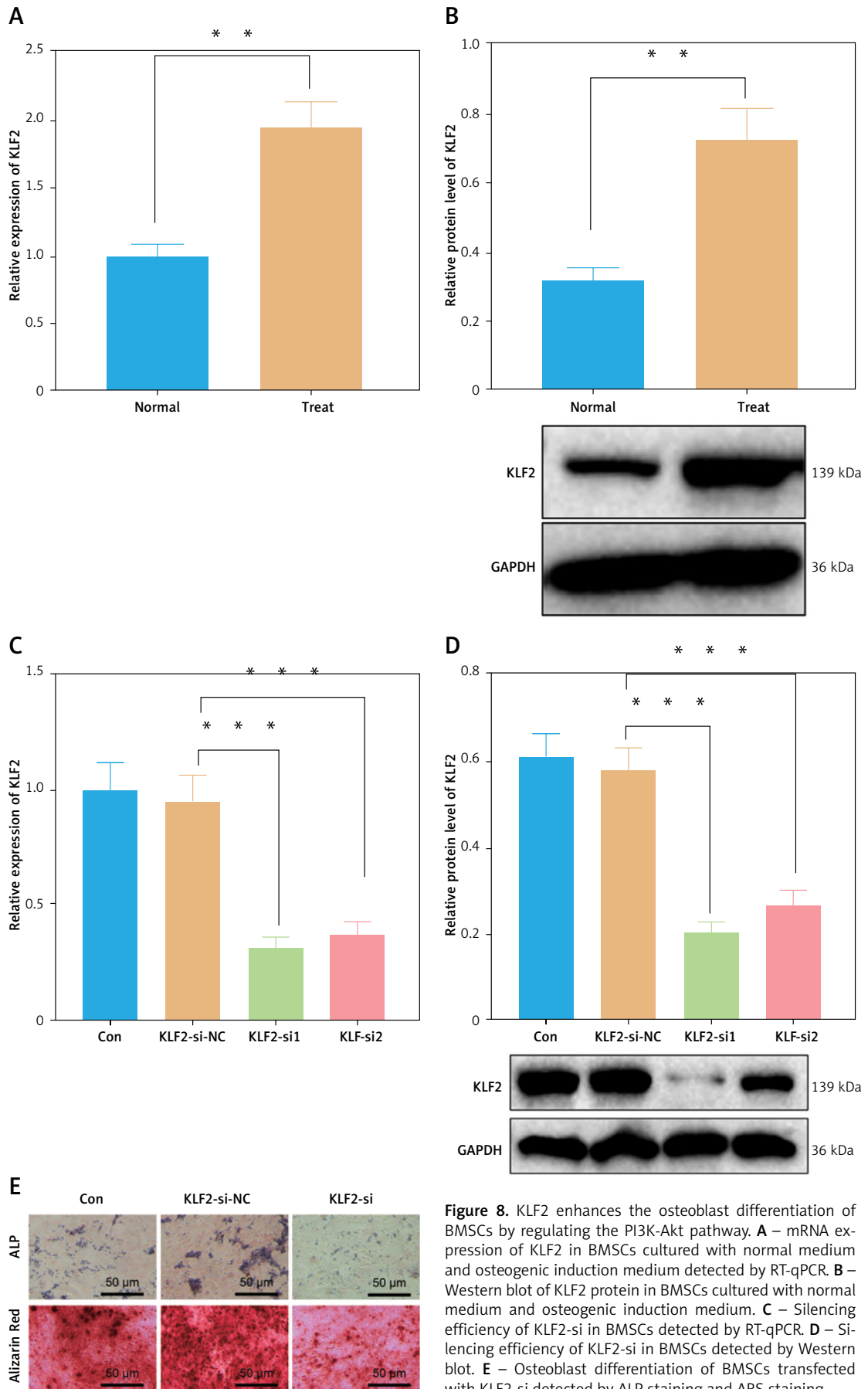


Figure 8. KLF2 enhances the osteoblast differentiation of BMSCs by regulating the PI3K-Akt pathway. **A** – mRNA expression of KLF2 in BMSCs cultured with normal medium and osteogenic induction medium detected by RT-qPCR. **B** – Western blot of KLF2 protein in BMSCs cultured with normal medium and osteogenic induction medium. **C** – Silencing efficiency of KLF2-si in BMSCs detected by RT-qPCR. **D** – Silencing efficiency of KLF2-si in BMSCs detected by Western blot. **E** – Osteoblast differentiation of BMSCs transfected with KLF2-si detected by ALP staining and ARS staining

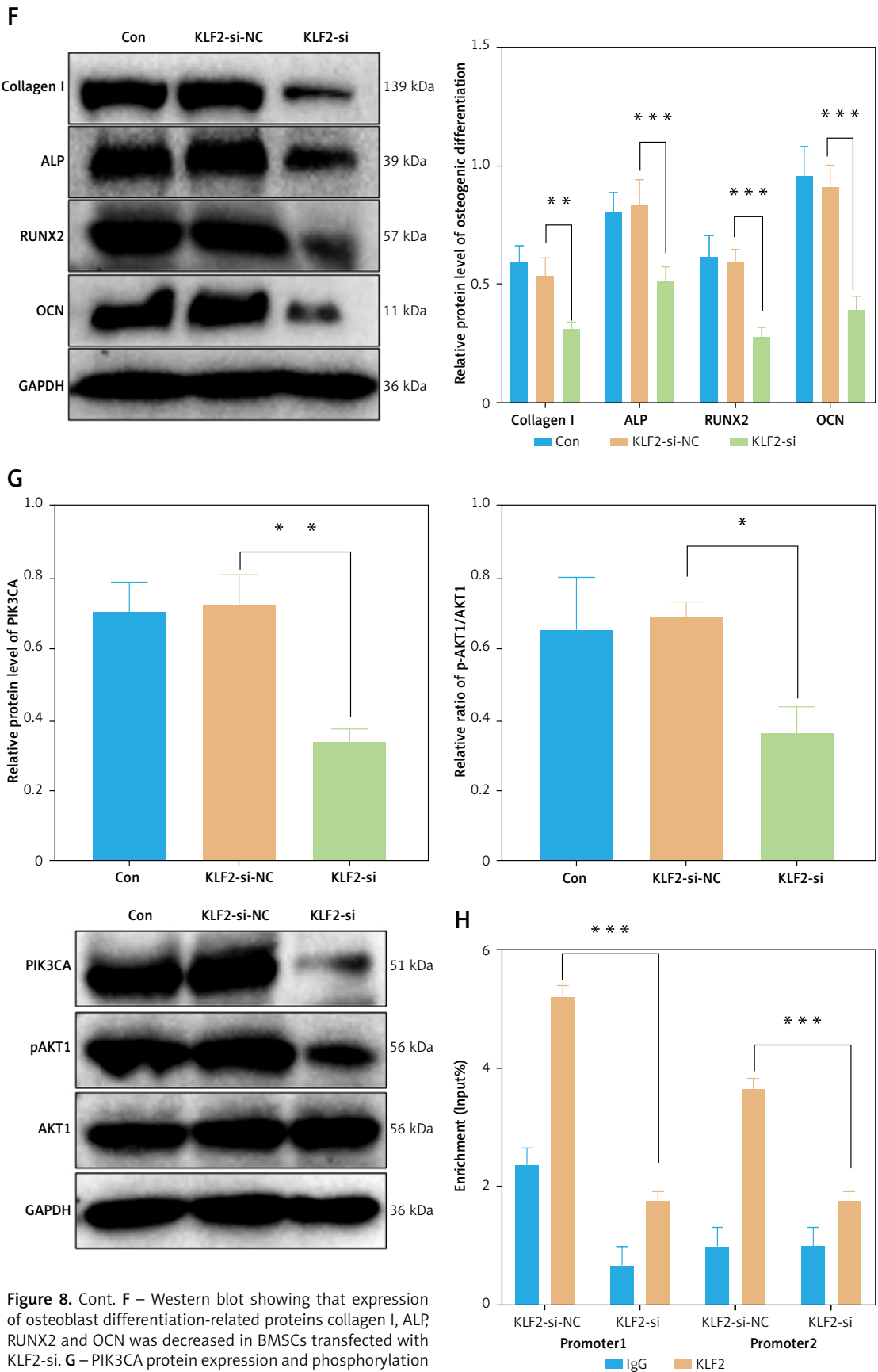


Figure 8. Cont. **F** – Western blot showing that expression of osteoblast differentiation-related proteins collagen I, ALP, RUNX2 and OCN was decreased in BMSCs transfected with KLF2-si. **G** – PIK3CA protein expression and phosphorylation level of Akt1 in BMSCs transfected with KLF2-si detected by Western blot. **H** – Binding of KLF2 to the promoter region of PIK3CA analyzed by ChIP assay. * $p < 0.05$, ** $p < 0.01$.

informatics and experimental analyses. The study identified the core gene PIK3CA involved in regulation of the PI3K-Akt pathway in PMO, and its expression was beneficial for the osteoblast differentiation of BMSCs, regulated by the transcription factor KLF2. The findings provide a starting point for future research on MSC-based therapies to treat PMO.

We performed differential analysis to screen for DEGs in PMO, and WGCNA singled out a green core module. A total of 197 genes were obtained as candidate ones in PMO, and combined with GO and KEGG enrichment analyses, PIK3CA was further identified as the core gene of the PI3K-Akt pathway for affecting PMO. Notably, PIK3CA was reported to be a pivotal protein that might regulate osteoporosis progression [15]. PIK3CA could be regulated by Jiawei Buguzhi Pills and could play a therapeutic role in PMO [31]. Activated PIK3CA/Akt/GSK3 β / β -catenin signaling by icariin could exert a protective function against glucocorticoid-induced osteoporosis [16]. Additionally, PIK3CA activation mutation could augment osteoblast differentiation in macrodactyly-derived BMSCs by regulating the PI3K/Akt/mTOR pathway [32]. These studies can provide support for our findings regarding the potential role of PIK3CA in PMO.

We further found in the present study that BMSCs could secrete the transcription factor KLF2 to increase the transcription of PIK3CA and enhance osteoblast differentiation of BMSCs. KLF2 can maintain the stemness of MSCs in bone regeneration [29] and result in the self-renewal of human BMSCs [33]. Prior research demonstrated that the culture of human BMSCs with the medium could increase the expression of KLF2 [34]. Intriguingly, KLF2 expression can be elevated by BMSC-derived EVs carrying miR-15b, which facilitates osteoblast differentiation [18]. Moreover, the p53/KLF2 axis dependent on JMJD3 was found to be activated in the presence of BMSC-derived EVs, thereby alleviating hypoxic-ischemic brain injury in neonatal mice [35]. To our knowledge, the regulatory effect of KLF2 on the PI3K-Akt pathway has been previously revealed. For instance, resveratrol-regulated KLF2 expression activates the PI3K/Akt pathway, protecting Min6 cells against uric acid-induced injury [36]. Unlike our results, the previous research failed to investigate the direct regulatory effect of KLF2 on PIK3CA. The function of KLF2 in osteoblast differentiation has been increasingly highlighted. Overexpressed KLF2 in MC3T3-E1 cells results in increased levels of osteoblast differentiation markers, including *Alp*, *Osx*, and *Ocn*, and regulates *RUNX2* to facilitate osteoblast differentiation [37]. Additionally, KLF2 demethylation by *Kdm3a* stimulates osteoblast differentiation in osteoporosis [38]. Therefore,

BMSC-secreted KLF2 could activate the PIK3CA-mediated PI3K-Akt pathway to promote osteoblast differentiation in PMO.

Furthermore, our study demonstrated that the PI3K-Akt pathway participated in osteoblast differentiation in PMO. QingYan formula extracts had a potential alleviatory effect on PMO, which was achieved partially by activating the PI3K-Akt pathway in osteoblasts [39]. Intriguingly, the activated PI3K-Akt pathway suppresses chaperone-mediated autophagy activity of rat BMSCs, thereby promoting the osteoblast differentiation of rat BMSCs [40]. Furthermore, upregulated expression of the PI3K-Akt pathway-related genes by beraprost aids in enhancing the differentiation of mouse BMSCs to ameliorate PMO [41]. Inhibition of the PI3K-Akt pathway by miR-320a can alleviate the development of PMO [42]. The results of these reports are all consistent with ours, showing the participation of the PI3K-Akt pathway in osteoblast differentiation in PMO.

Taken together, the results of the present study demonstrate that BMSCs effectively alleviated PMO by secreting the transcription factor KLF2, which increased PIK3CA expression and activated the PI3K-Akt pathway to promote osteoblast differentiation. The study provides a foundation for future research on the role of PIK3CA and KLF2 in promoting osteoblast differentiation in MSCs and their potential in developing novel therapeutic targets. The study also highlights the importance of investigating the underlying molecular mechanisms in the use of MSCs as a source of cell-based therapy for PMO. However, the study has certain limitations such as its focus on molecular mechanisms only, absence of clinical trials, and lack of investigation of other transcription factors and their interaction with PIK3CA. Future studies could focus on exploring the potential of MSC-based therapy in clinical trials and identifying novel targets for osteoblast differentiation, e.g., targeting other transcription factors that interact with PIK3CA. Additionally, further research could aid in identifying potential strategies to optimize this therapy for patients with osteoporosis.

Acknowledgments

We acknowledge and appreciate our colleagues for their valuable efforts and comments on this study.

Funding

No external funding.

Ethical approval

Not applicable.

Conflict of interest

The authors declare no conflict of interest.

Availability of data and materials

The data that support the findings of this study are available in the manuscript and supplementary materials.

References

- Shevroja E, Cafarelli F, Guglielmi G, Hans D. DXA parameters, trabecular bone score (TBS) and bone mineral density (BMD), in fracture risk prediction in endocrine-mediated secondary osteoporosis. *Endocrine* 2021; 74: 20-8.
- Shi H, Jiang X, Xu C, Cheng Q. MicroRNAs in serum exosomes as circulating biomarkers for postmenopausal osteoporosis. *Front Endocrinol (Lausanne)* 2022; 13: 819056.
- Migliorini F, Maffulli N, Colarossi G, Eschweiler J, Tingart M, Betsch M. Effect of drugs on bone mineral density in postmenopausal osteoporosis: a Bayesian network meta-analysis. *J Orthop Surg Res* 2021; 16: 533.
- Migliorini F, Giorgino R, Hildebrand F, et al. Fragility fractures: risk factors and management in the elderly. *Medicina (Kaunas)* 2021; 57: 1119.
- Postmenopausal osteoporosis. *N Engl J Med* 2016; 374: 1797.
- Bijelic R, Milicevic S, Balaban J. Risk factors for osteoporosis in postmenopausal women. *Med Arch* 2017; 71: 25-8.
- Migliorini F, Maffulli N, Spiezia F, Peretti GM, Tingart M, Giorgino R. Potential of biomarkers during pharmacological therapy setting for postmenopausal osteoporosis: a systematic review. *J Orthop Surg Res* 2021; 16: 351.
- Migliorini F, Colarossi G, Baroncini A, Eschweiler J, Tingart M, Maffulli N. Pharmacological management of postmenopausal osteoporosis: a level i evidence based - expert opinion. *Expert Rev Clin Pharmacol* 2021; 14: 105-19.
- Deng YX, He WG, Cai HJ, et al. Analysis and validation of hub genes in blood monocytes of postmenopausal osteoporosis patients. *Front Endocrinol (Lausanne)* 2021; 12: 815245.
- Noronha-Matos JB, Correia-de-Sa P. Mesenchymal stem cells ageing: targeting the "purinome" to promote osteogenic differentiation and bone repair. *J Cell Physiol* 2016; 231: 1852-61.
- Chen W, Chen X, Chen AC, et al. Melatonin restores the osteoporosis-impaired osteogenic potential of bone marrow mesenchymal stem cells by preserving SIRT1-mediated intracellular antioxidant properties. *Free Radic Biol Med* 2020; 146: 92-106.
- Luo ZW, Li FX, Liu YW, et al. Aptamer-functionalized exosomes from bone marrow stromal cells target bone to promote bone regeneration. *Nanoscale* 2019; 11: 20884-92.
- Migliorini F, Maffulli N, Spiezia F, Tingart M, Maria PG, Riccardo G. Biomarkers as therapy monitoring for postmenopausal osteoporosis: a systematic review. *J Orthop Surg Res* 2021; 16: 318.
- Lai K, Killingsworth MC, Lee CS. Gene of the month: PIK3CA. *J Clin Pathol* 2015; 68: 253-7.
- Liu B, Wang A, Cao Z, Li J, Zheng M, Xu Y. Mechanism of pilose antler in treatment of osteoporosis based on network pharmacology. *J Healthc Eng* 2022; 2022: 5298892.
- Hu J, Mao Z, He S, et al. Icaritin protects against glucocorticoid induced osteoporosis, increases the expression of the bone enhancer DEC1 and modulates the PI3K/Akt/GSK3beta/beta-catenin integrated signaling pathway. *Biochem Pharmacol* 2017; 136: 109-21.
- Jha P, Das H. KLF2 in regulation of NF-kappaB-mediated immune cell function and inflammation. *Int J Mol Sci* 2017; 18: 2383.
- Li Y, Wang J, Ma Y, et al. MicroRNA-15b shuttled by bone marrow mesenchymal stem cell-derived extracellular vesicles binds to WWP1 and promotes osteogenic differentiation. *Arthritis Res Ther* 2020; 22: 269.
- Kim I, Kim JH, Kim K, Seong S, Kim N. The IRF2BP2-KLF2 axis regulates osteoclast and osteoblast differentiation. *BMB Rep* 2019; 52: 469-74.
- Ebert R, Meissner-Weigl J, Zeck S, et al. Probenecid as a sensitizer of bisphosphonate-mediated effects in breast cancer cells. *Mol Cancer* 2014; 13: 265.
- Sako K, Fukuhara S, Minami T, et al. Angiotensin-1 induces Kruppel-like factor 2 expression through a phosphoinositide 3-kinase/AKT-dependent activation of myocyte enhancer factor 2. *J Biol Chem* 2009; 284: 5592-601.
- Huang X, Hao S, Liu J, et al. The ubiquitin ligase Peli1 inhibits ICOS and thereby Tfh-mediated immunity. *Cell Mol Immunol* 2021; 18: 969-78.
- Malakoti F, Zare F, Zarezadeh R, et al. The role of melatonin in bone regeneration: a review of involved signaling pathways. *Biochimie* 2022; 202: 56-70.
- Zhao F, Xu Y, Ouyang Y, et al. Silencing of miR-483-5p alleviates postmenopausal osteoporosis by targeting SATB2 and PI3K/AKT pathway. *Aging (Albany NY)* 2021; 13: 6945-56.
- Gong L, Tang Y, An R, Lin M, Chen L, Du J. RTN1-C mediates cerebral ischemia/reperfusion injury via ER stress and mitochondria-associated apoptosis pathways. *Cell Death Dis* 2017; 8: e3080.
- He X, Chai P, Li F, et al. A novel lncRNA transcript, RBAT1, accelerates tumorigenesis through interacting with HNRNPL and cis-activating E2F3. *Mol Cancer* 2020; 19: 115.
- Zhang Y, Cao X, Li P, et al. PSMC6 promotes osteoblast apoptosis through inhibiting PI3K/AKT signaling pathway activation in ovariectomy-induced osteoporosis mouse model. *J Cell Physiol* 2020; 235: 5511-24.
- Kou J, Zheng X, Guo J, Liu Y, Liu X. MicroRNA-218-5p relieves postmenopausal osteoporosis through promoting the osteoblast differentiation of bone marrow mesenchymal stem cells. *J Cell Biochem* 2020; 121: 1216-26.
- Zhou Y, Liu C, He J, et al. KLF2(+) stemness maintains human mesenchymal stem cells in bone regeneration. *Stem Cells* 2020; 38: 395-409.
- Xu R, Shen X, Xie H, et al. Identification of the canonical and noncanonical role of miR-143/145 in estrogen-deficient bone loss. *Theranostics* 2021; 11: 5491-510.
- Yuan X, Wu Y, Yang K, Liu H, Zhang G. Exploring the effect of Jiawei Buguzhi Pills on TGF-beta-Smad pathway in postmenopausal osteoporosis based on integrated pharmacological strategy. *Evid Based Complement Alternat Med* 2021; 2021: 5556653.
- Cui H, Han G, Sun B, et al. Activating PIK3CA mutation promotes osteogenesis of bone marrow mesenchymal stem cells in macrodactyly. *Cell Death Dis* 2020; 11: 505.
- Wang H, Zhou Y, Yu D, Zhu H. Klf2 contributes to the stemness and self-renewal of human bone marrow stromal cells. *Cytotechnology* 2016; 68: 839-48.
- Zhou Y, Yu D, Zhu H. Optimization of culture condition of human bone marrow stromal cells in terms of purifi-

- cation, proliferation, and pluripotency. *In Vitro Cell Dev Biol Anim* 2014; 50: 822-30.
35. Luo H, Huang F, Huang Z, et al. microRNA-93 packaged in extracellular vesicles from mesenchymal stem cells reduce neonatal hypoxic-ischemic brain injury. *Brain Res* 2022; 1794: 148042.
 36. Xin Y, Zhang H, Jia Z, et al. Resveratrol improves uric acid-induced pancreatic beta-cells injury and dysfunction through regulation of miR-126. *Biomed Pharmacother* 2018; 102: 1120-6.
 37. Hou Z, Wang Z, Tao Y, et al. KLF2 regulates osteoblast differentiation by targeting of Runx2. *Lab Invest* 2019; 99: 271-80.
 38. Wu JC, Sun J, Xu JC, Zhou ZY, Zhang YF. Down-regulated microRNA-199a-3p enhances osteogenic differentiation of bone marrow mesenchymal stem cells by targeting Kdm3a in ovariectomized rats. *Biochem J* 2021; 478: 721-34.
 39. Wang D, Zhang Y, Xu X, et al. YAP promotes the activation of NLRP3 inflammasome via blocking K27-linked polyubiquitination of NLRP3. *Nat Commun* 2021; 12: 2674.
 40. He Q, Qin R, Glowacki J, et al. Synergistic stimulation of osteoblast differentiation of rat mesenchymal stem cells by leptin and 25(OH)D(3) is mediated by inhibition of chaperone-mediated autophagy. *Stem Cell Res Ther* 2021; 12: 557.
 41. Zheng HL, Xu WN, Zhou WS, et al. Beraprost ameliorates postmenopausal osteoporosis by regulating Nedd4-induced Runx2 ubiquitination. *Cell Death Dis* 2021; 12: 497.
 42. Kong Y, Nie ZK, Li F, Guo HM, Yang XL, Ding SF. MiR-320a was highly expressed in postmenopausal osteoporosis and acts as a negative regulator in MC3T3E1 cells by reducing MAP9 and inhibiting PI3K/AKT signaling pathway. *Exp Mol Pathol* 2019; 110: 104282.